Challenges for single-crystal (SX) crack cladding

Boris Rottwinkel[a,]*, Luiz Schweitzer[a], Christian Noelke[a], Stefan Kaierle[a],
Volker Wesling[a]

[a]*Laser Zentrum Hannover e.V., Hollerithallee 8, 30419 Hanover, Germany*

Abstract

The formation of cracks in single-crystal (SX) turbine blades is a common problem for aero-engines. If cracks are located under the tip-area, the blade-repair is not possible. A new method to repair these cracks is to clad with single-crystal-technology. To reduce the loss of material and working time, notches are used to remove the affected crack zone. The used notch geometries must be weldable and also permit the material solidification in the same oriented plane as the original microstructure. For that, a thermal gradient has to be introduced in order to guide the grain growth. The process characteristics of laser cladding, such as small local heat input and controlled material supply, make it an efficient process to fill the notch. However, there are challenges to achieve a SX structure without cracks and pores. The unstable energy distribution may result in a polycrystalline structure. Current achievements and further challenges are presented in this paper.

Keywords: crack cladding; single-crystal cladding; aero engine repair

1. Maintenance of aero engines – SX-repair

The volume of the blade repair market all over the world is immense. According to Rupp (2001), aircraft engines servicing accounts to about 45 percent of the total cost of the whole engine aircraft maintenance. Maintenance of the single crystal turbine blades, which are used in Stage 1 or in today´s state of the art engines also in Stage 2 of the high-pressure-turbine (HPT), is still a complex process.

Due to the high thermal and mechanical stresses during operation, these parts are mainly manufactured in a complex casting procedure to achieve a single-crystal microstructure. The specific morphology is oriented along the direction of axial stresses. This orientation increases the operating limits significantly compared to polycrystalline blades also used in aero-engines.

* Corresponding author. Tel.: +49-511-2788-234; fax: +49-511-2788-100 .
   E-mail address: b.rottwinkel@lzh.de

Jayakumar et. al. (1999) identified, that the most common failure case in turbine blades is creep. They also showed that this is also the life limiting factor. Due to significant reduction of grain boundaries for epitaxial orientation, the single-crystal structures withstand creep at higher temperature levels then common structures. Grain boundaries within the microstructure can initiate failure mechanisms, which decrease the high temperature strength that causes creep failure. To avoid nucleation in the laser cladding process, Kurz et al. (2001) postulates the columnar to equiaxed transition (CET). This transition correlates the effect of the thermal gradient to the solidification speed. The needed thermal gradient to reach columnar solidification was calculated by Gaeumann et al. (1999). This identified limits enabled the growth of equiaxed grains within the molten material. Also Gaeumann (1999) analysed the processing maps of single crystal manufacturing with the use of a preheating. This preheating on the one hand reduced the thermomechanical stresses and so avoid the formation of hot and cold cracks. This was also shown before by David et al (1997).

In the present work, the laser crack cladding process was considered for the similar SX-repair of single-crystalline blades made of CMSX-4. Santos et al. (2010) were able to clad single-crystal structures on flat samples by using two different alloys. The use of Rene N4 powder on CMSX-4 substrate showed a single-crystal microstructure orientation. Gaeumann et. al. (2001) were able to clad crack free single track-volumes on a mono crystalline CMSX-4 substrate to rebuild single-crystal structures. To clad single tracks, like small walls, Gaeumann claim three main steps for the single-crystal formation:

First, the temperature of the used substrate should be as low as possible. Second, preheating should be avoided. Final, avoid overheating of the melt pool by using a laser power control.

Those three recommendations could be proven during our researches (Fig. 1a). In Fig. 1b, the substrate was preheated to show the effect on the crystal formation using a preheated substrate.
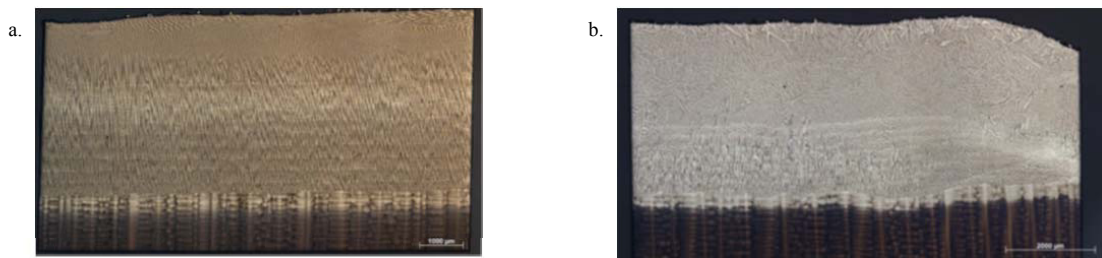

Fig. 1. SX-cladding without (a) and with (b) preheating.

During the process, a water cooled platform was used to reduce the temperature of the substrate to 18°C. For the laser cladding process, a diode laser with maximum power of 680 W, a wavelength of 940/980 nm and a fibre diameter of 400 μm were used. The used process parameters are summarized in Table 1.

Table 1. Single-crystal clad parameter.

	Without preheating	With preheating
Feed rate [mm/min]	100	100
Powder feed rate [g/min]	3	3
Laser power [W]	100 – 350	100 – 350
Temperature at molten bath [°C]	1400	1400
Preheat temperature [°C]	-	650

To repair turbine blades with cracks, as shown in Fig. 2 the cladding process cannot be performed with a single track. To rebuild large areas like tips on blades, the process must be extended to multi-track cladding per layer without crack formation. The formation of cracks during notch cladding was an important fact to be analyzed. It was explicit that the notch geometry turns the SX clad into a complex system due to heat distribution and residual stresses in the region.

The introduction of a notch in the substrate is a method developed to optimize the crack repair on the tip of

turbine blades. It consists of cutting the damaged region with a weldable geometry in order to remove the crack and rebuilt it. On the other hand, the clad complexity is increased due to the energy distribution inside the notch. The heat flow occurs no longer in one dimension, but in two, since the heat propagates to the lateral area as well. This phenomenon generates a region suitable for crack formation due to residual stresses resulting from tensile and compressive strength. In order to reduce stresses, a thermal induction is used to preheat the substrate by means of an electromagnetic field. This decreases the temperature gradient on the one hand, but reduces the residual stress.

Fig. 2. Damage on turbine blade tip.

Since the SX alloys do not contain grain boundary hardening elements, it is necessary that the reshaping technique also results in a single-crystal for the required material properties to avoid cracking. To avoid the formation of grains, the thermal gradient must be formed well. During laser cladding, the thermal gradient is orientated to the cold substrate and at the clad´s top rectangular to the clad direction. Using multi-track cladding, these orientations will be extended to multi direction. These directions are influenced by the clad tracks next to each other. To avoid more thermal gradient orientations, long processing times or even high energy levels should be avoided.

On the other hand, for the repair of cracked blades, the thermal expansion of nickel-base superalloys results in high tensile stresses in the cladded notch. To avoid this, preheating of the samples shows advantages, even if this was negated by Gaeumann. To overcome this problem, a specific temperature distribution is required to enable a heated and a cooled front that controls the direction of solidification.

2. Method

To reduce the complexity of the test set-up, samples with dimensions of 30x30x2 mm³ were used (Fig. 3). These samples were single crystal cast and made of the nickel base superalloy CMSX-4. The samples were cast by PCC Airfoil and manufactured according to the same requirements as turbine blades, which have a defined grain orientation to be followed by the new clad. X-ray analysis was done to detect any failures.

In the future process, cracks should be detected and repaired on blade geometries. To simulate this process, the needed clad notch geometries were prepared with laser cutting or mechanical milling.

The experimental test bench consists basically of three components: cooling plates, inductive preheating and precision elevator. The substrate was fixed between the two cooling plates, which permitted the fast heat exchange between the surfaces.
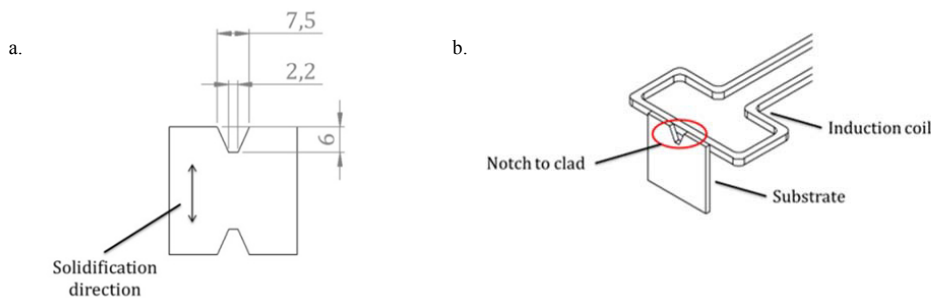

Fig. 3. Specimen (a) and process set-up (b).

An inductive coil, which heats up the area part of the substrate, was located next to the notch. The elevator moved the system down in order to correct the molten bath position relative to the induction coil. Both, induction

coil and cooling plates, defined the required thermal gradient respectively the direction of solidification.

The notch design shown in Fig. 3a was used for these cladding processes. Several other geometries were evaluated and the resultant geometry corresponds best.

The used strategy to perform the experiments by filling up the notch completely was a multi-layer technique as shown in Fig. 4, with three tracks side by side. The strategy showed good results concerning powder efficiency and process speed.
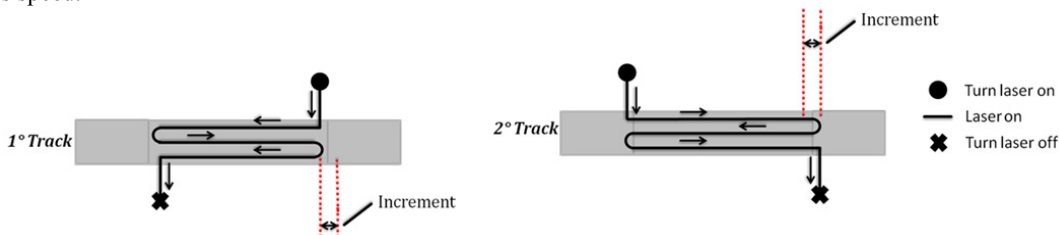
Fig. 4. Cladding strategy.

The cladding process were done starting from two directions, in order to build up a symmetric clad. For every new layer an increment was added on the lateral component between each clad in order to compensate the notch geometry according to the clad growth. After each clad the precision elevator corrected the working surface height in order to remain in the laser focus and also at the same referential position to the induction coil.

3. Results

The first trial corresponds to a replication of the parameters obtained in a basis research (see Table 1), which resulted in the epitaxial solidification of clads on planar surfaces. It was executed and repeated with and without the preheating to evaluate its influence on the clad formation, as presented in Table 2.

Table 2. notch parameters.

Sample	Focus radius [mm]	Feed rate [mm/min]	Cooling dist. [mm]	Temp. [°C]	Powder [g/min]	Preheating [W/°C]
N1	0.396	100	4	1400	3	-
N2	0.396	100	4	1400	3	2000/650

The metallographic results are presented in Fig. 5 and Fig. 6, which corresponds to the longitudinal cut on the notch of each specimen and the cross sectional cut from the clad on the top.

The first sample corresponds to the clad without preheating (N1 - Fig. 5) and the second with it (N2 - Fig. 6). The microstructure of N1 approximates to the single-crystal solidification even in the cross section, but there are cracks and pores in it. The thermal expansion of the material resulted in the formation of stresses which initiated cracks. Their origin was at the top of the clad. Guided along the few grain boundaries, cracks stopped at the original SX-structure.
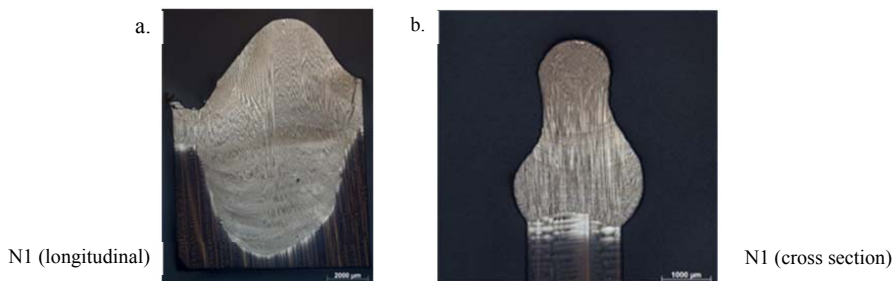
a.   b.

N1 (longitudinal)   N1 (cross section)

Fig. 5. crack-cladded sample N1.

Sample N2 (Fig. 6) showed a crack free clad with equiaxed solidification. Since the preheating is the only difference between, it is reasonable to assume that the microstructure is vulnerable to the thermal induction influence.
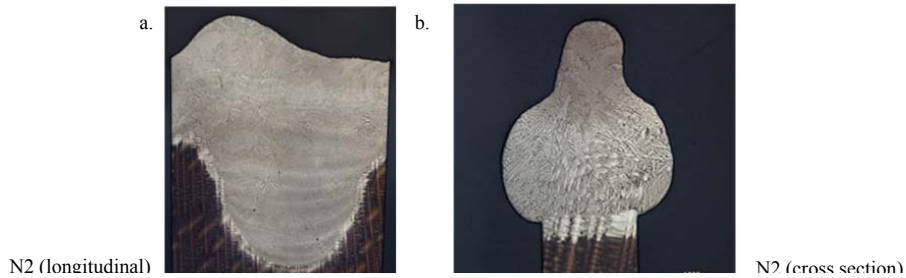

a. b.

N2 (longitudinal) N2 (cross section)

Fig. 6. Crack-cladded sample N2.

These two samples show clearly that preheating has a strong influence on the grain growth during solidification inside the notch. Additionally the crack formation through the thermal expansion ratio of the nickel-base superalloys could be shown. It is important to consider that the thermal induction, despite providing a crack free microstructure, is unsuitable for the formation of a single-crystal clad. However, trials without preheating have shown cracks, which are also unacceptable. This was also demonstrated before by Gaeumann (1999) for single layer clads

To reduce crack formation, parameters were changed to pursuit the formation of thinner layers in order to reduce the needed laser power and so the loss of the thermal gradient orientation. The preheating of the sample was skipped to reduce the temperature in the clad area. These small single crystal layers may be more resist against the residual stress indicated by thermal expansion. The used parameters are presented in Table 3. In the first samples N3 (see Fig. 7a) the powder injection was reduced to 1 g/min. This resulted in a lower laser power through reduced powder interactions and melting energy. The laser power was controlled using a PID-controller with a Sensortherm pyrometer to control the temperature of the clad pool to 1400°C. Melting temperature of the used alloy is about 1380 - 1400°C. Cracks could be detected as shown in Fig. 7. In sample N3 the powder ratio was set to 2 g/min. The rise of powder resulted also in formation of cracks. In N5 the feed rate was increased by 50 percent. Using an increased speed, the heat affected zone was decreased. Nevertheless, cracks occurred and the microstructure was polycrystalline.

To guide the thermal gradient more precise the focus radius was set to 0.671 mm. This should reduce the number of layers needed to fill the notch. As shown at specimen N6 (see Fig. 7b) cracks were detected as well.
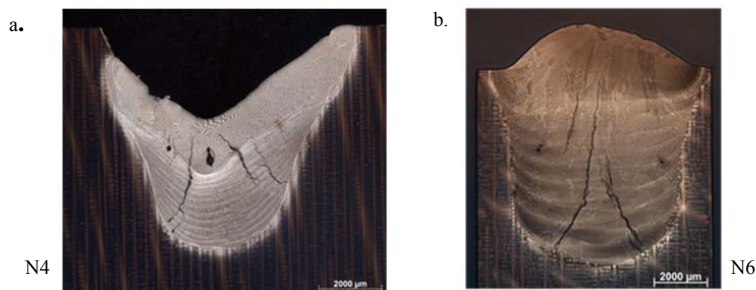

a. b.

N4 N6

Fig. 7. Notch samples N4 (a) and N6 (b).

Table 3. Notch process parameters.

Sample	Focus radius [mm]	Feed rate [mm/min]	Cooling dist. [mm]	Temp. [°C]	Powder [g/min]	Preheating [W/°C]
N3	0.396	100	4	1400	2	no
N4	0.396	100	4	1400	1	no
N5	0.396	150	4	1400	3	no
N6	0.671	100	4	1400	3	no

As shown in Fig. 7, thinner layers could be achieved in specimen N4. However, this was not efficient to avoid the crack formation. This damage may be linked with the energy distribution on the clad, which suffers from the mechanism described at the beginning of this chapter.

The results from the parameter studies lead to the conclusion that substrate preheating is needed to stabilize the upper region and prevent the residual stresses. For the experiments it is necessary to achieve a clad strategy in order to maintain the single-crystal structure and avoid cracks. The previous base parameters were used, as shown in Table 4, but with different approaches to use the thermal induction as preheating unit in order to avoid the polycrystalline microstructure.

Table 4. Parameter N7 - N12.

Sample	Focus radius [mm]	Feed rate [mm/min]	Cooling dist. [mm]	Temp. [°C]	Powder [g/min]	Preheating [max. W/°C]
N7	0.396	100	4	1400	3	2000/500
N8	0.396	100	4	1400	3	2000/650
N9	0.396	100	4	1400	3	2000/650
N10	0.396	100	no	1400	3	2000/650
N11	0.396	100	no	1400	3	no
N12	0.396	100	no	no PID	3	no

Fig. 7 presents the metallographic results according to the strategies described. The preheating was controlled by a PID-Controller to set the required temperature. Sample N7 (Fig. 8a) show the result for a low preheating temperature. The influence from the thermal induction was reduced and the analysis shows the initial formation of a single-crystal microstructure in the bottom region. In order to reduce even more the action of the thermal induction, the inductive preheating was shut down directly after (N8) and before (N9) the cladding process. In sample N8 the device is turned off after the clad, but it is not efficient due to the high cooling rate and fast solidification, which resulted in a polycrystalline microstructure. However, N9 showed an improvement in the microstructure since there was no magnetic field acting during the process. These magnetic fields could affect the dendrites orientation or even break the dendrites. The effect of breaking dendrites was also shown by Ren et al. (2013). This has to be proven for our setup by Scanning Electron Microscope (SEM)-analysis.

The reduction of the cooling rate should keep the preheating temperature for longer time before it is completely cooled down. Parameter setup N10 did not use a direct cooling interface. The sample was fixed on top of the cooling plates to cool the sample indirectly. Cracks still occurred as shown in Fig. 9b.
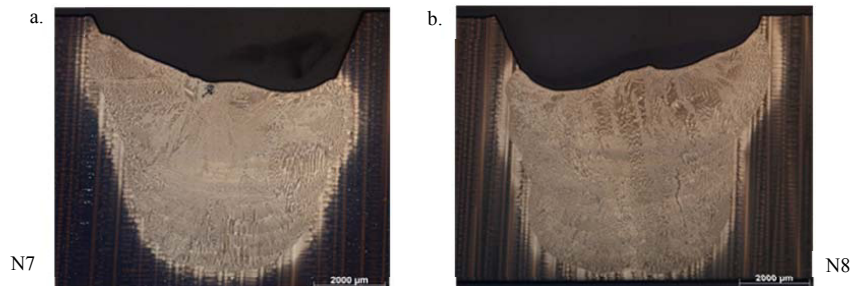

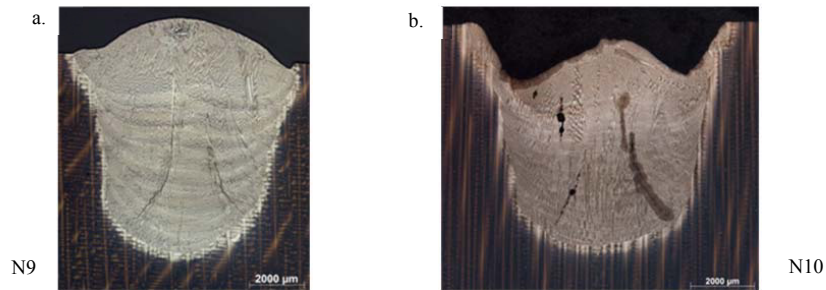Fig. 8. notch samples N7 (a) and N8 (b).

Fig. 9. Notch samples N9 (a) and N10 (b).

To evaluate the new cooling strategy, specimen N11 (Fig. 10a) was tested without the preheating as shown in Table 4. The single-crystal microstructure was achieved for the most part of the clad, but there were cracks left on the upper left region.

The last sample N12 (Fig. 10b) was realized with a different strategy to achieve the molten bath temperature. The laser power was no longer controlled by PID. Also preheating was not used. The first two layers were performed with 300 W, the following with 350 W. A crack free clad with mainly polycrystalline microstructure was reached.
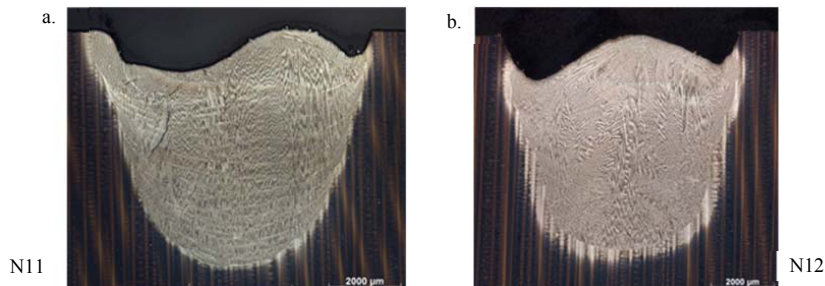

Fig. 10. notch samples N11 (a) and N12 (b).

The detected cracks were analysed using SEM in order to evaluate and discover their origin (Fig. 11). A crack is marked by a red circle. The white matrix corresponds to the γ-matrix and the black spots to the γ'-phase. The faster growth of γ'-phase generates a more fragile region in which the crack starts. There are two possible reasons for the formation of such regions: overheating or uneven heat distribution. Both phenomena produce a region more suitable for the growth of γ'-phases. Once the crack begins, the SX microstructure is convenient for the growth since there are no grain barriers to stop it. For this reason most of cracks cross the complete clad. The defects may be characterized as cold cracking according to the detailed view in SEM.
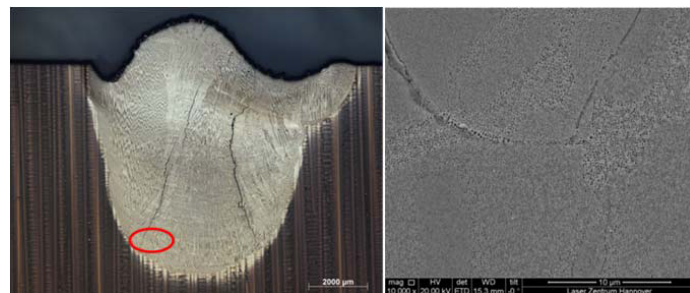

Fig. 11. SEM analysis.

4. Conclusion

Within the shown parameter study it was not possible to produce a complete single-crystalline clad. The results consists either the SX microstructure with cracks using preheating or the polycrystalline crack free with preheating. In order to discover a point between these two problems, several clad strategies have been evaluated. They basically did not differ on process parameters, but how the preheating and cooling affected the system. Since the preheating is capable to eliminate the crack formation, the methods tested are trials to preheat the substrate with the thermal induction, but reduce the effects of the electromagnetic field. For that a few strategies were performed. The thermal induction was set far from the substrate, shut down after each clad, shut down before each clad, the cooling was reduced and even the molten bath temperature control was disabled. The temperature control was used at sample N11, which present a small crack and almost completely SX-microstructure. By N12 the laser power was not controlled and the resultant specimen has no crack, but is mostly polycrystalline.

The energy in the processes (N11 and N12) was defining the microstructure and the presence of cracks. Using SEM, the origin of cracks occurring in regions where the γ'-phase has achieved larger dimensions could be localized. Since it corresponds to the hard and also brittle part of the microstructure, such formation is fragile and suitable for the crack beginning. The SX also provide a microstructure suitable to the crack growth as it has no grain boundary to stop it. Another characteristic observed on the clad formation is the influence of the electromagnetic field, generated by the thermal induction, on the microstructure. Parameter studies have to evaluate the effect in further studies.

The main objective of these experiments has been to evaluate which from these key parameters influences the clad problems. From the test series done it can be assumed that the adequate adjusting of the indirect cooling is the most promising parameter to achieve improved results.

Acknowledgments

References

Rupp, O. (2001) Instandhaltungskosten bei zivilen Strahltriebwerken. Deutscher Luft- und Raumfahrtkongress 2001, DGLR 2001-008,

Jayakumar, T.; Muralidharan, N.G.; Raghu, N.; Kasiviswanathan, K.V.; Raj, B. (1999) Failure Analysis towards Reliable Performance of Aero-Engines. Defence Science Journal, Vol49, No 4, pp. 3 11-3 16

Santos, E. C.; Kida, K.; Carroll, P. & Vilar, R. (2010), Optimization of Laser Deposited Ni-Based Single Crystal Superalloys Microstructure. Advanced Materials Research, Volumes 154-155, Pages 1405-1414

Gaeumann, M.; Bezençon, C.; Canalis, P. & Kurz, W. (2001), Single-crystal laser deposition of superalloys: Processing-microstructure maps. Acta Mater. Volume 49, Pages 1051–1062

Gaeumann, M.; Henry, S.; Cléton, F.; Wagnière, J.-D. & Kurz, W. (1999) Epitaxial laser metal forming: analysis of microstructure formation. Materials Science and Engineering: A, Volume 271, Pages 232–241

Gaeumann, M. (1999) Epitaxial laser metal forming of a single crystal superalloy. Thesis, These n° 1907 École Polytechnique Fédérle de Lausanne

David, S. A.; Vitek, J. M.; Babu, S. S.; Boatner, L. A.; Reed, R. W. (1997) Weliding of nickel base superalloy single crystals. Science and Technology of Welding and Joining, Volume 2 Issue 2, pp. 79-88

Kurz, E.; Bezenvon, C. & Gaeumann, M. (2001) Columnar to equiaxed transition in solidification processing. Science and Technology of Advanced Materials, Volume 2, Pages 185-191

Ren, W.; Lu, L.; Yuan, G.; Xuan, W.; Zhong, Y.; Yu, J., Ren, Z. (2013) The effect of magnetic field on precipitation phase of single-crystal nickel-base superalloy during directional solidification. Material Letter 100, Pages 223-226